Targeted downregulation of N-acetylgalactosamine 4-sulfate 6-O-sulfotransferase (GalNAc4S6ST) significantly mitigates chondroitin sulfate proteoglycan (CSPG) mediated inhibition

Lohitash Karumbaiah[1], **Sanjay Anand**[1], **Rupal Thazhath**[2], **Yinghui Zhong**[1], **Robert J. McKeon**[3], and **Ravi V. Bellamkonda**[1,*]

[1]Wallace H. Coulter Department of Biomedical Engineering at Georgia Institute of Technology and Emory University School of Medicine, Atlanta, GA 30332

[2]Department of Biology, Georgia Institute of Technology, Atlanta, GA 30332

[3]Department of Cell Biology, Emory University, GA 30322

Abstract

Chondroitin Sulfate-4,6 (CS-E) glycosaminoglycan (GAG) upregulation in astroglial scars is a major contributor to CS proteoglycan (CSPG) mediated inhibition (Gilbert et al. 2005). However, the role of N-acetylgalactosamine 4-sulfate 6-O-sulfotransferase (GalNAc4S6ST) catalyzed sulfation of CS-E, and its contribution to CSPG mediated inhibition of CNS regeneration remains to be fully elucidated. Here, we used *in situ* hybridization to show localized upregulation of GalNAc4S6ST mRNA after CNS injury. Using *in vitro* spot assays with immobilized CS-E, we demonstrate dose dependent inhibition of rat embryonic day 18 (E18) cortical neurons. To determine whether selective downregulation of CS-E affected the overall inhibitory character of extracellular matrix produced by reactive astrocytes, single [against (chondroitin 4) sulfotransferase 11 (C4ST1) or GalNAc4S6ST mRNA) or double (against C4ST1 and GalNAc4S6ST mRNA] siRNA treatments were conducted and assayed using quantitative real-time PCR (qRT-PCR) and high performance liquid chromatography (HPLC) to confirm the specific downregulation of CS-4S GAG (CS-A) and CS-E. Spot and Bonhoeffer stripe assays using astrocyte conditioned media (ACM) from siRNA treated rat astrocytes showed a significant decrease in inhibition of neuronal attachment and neurite extensions when compared to untreated and TGFα treated astrocytes. These findings reveal that selective attenuation of CS-E via siRNA targeting of GalNAc4S6ST significantly mitigates CSPG mediated inhibition of neurons, potentially offering a novel intervention strategy for CNS injury.

Keywords

glycosaminoglycan; CS-E; astroglial scar; CNS repair; axon regeneration

Introduction

CSPGs are a family of extracellular matrix (ECM) proteins that play important roles in controlling neuronal migration and pathfinding (Grimpe and Silver 2002; Matthews et al. 2002; Snow et al. 1990; Sugahara and Mikami 2007). Structurally, they consist of a core

*Correspondence should be addressed to: Ravi V. Bellamkonda, PhD, GCC Distinguished Scholar &Professor, Department of Biomedical Engineering, Georgia Institute of Technology/Emory University, 3108 UA Whitaker Bldg., 313 Ferst Drive, Atlanta, GA 30332, Phone: 404.385.5038; Fax: 404.385.5044; ravi@gatech.edu.

protein to which are attached GAG side chains made up of repeating CS-disaccharide units (D-glucuronic acid (β1→3) *N*-acetyl-D-galactoseamine) (Lamberg and Stoolmiller 1974). CS-GAG chains are tethered to a serine residue on the core protein via a Xylose-galactose-galactose-glucoronic acid tetrasaccharide linking region, which is post-translationally added by the action of specific glycosyltransferases (Baker et al. 1972; Helting and Roden 1969a; Schwartz and Roden 1974; Schwartz and Roden 1975; Schwartz et al. 1974; Stoolmiller et al. 1972). Addition of the glucuronic acid residue in the tetrasaccharide linkage, and its subsequent addition along with N-acetylgalactosamine to form repeating CS-disaccharide units are catalyzed by two separate glucuronyl transferases and N-acetylgalactosaminyltransferases respectively (Helting and Roden 1969b; Rohrmann et al. 1985). CS-GAGs are sulfated by CS sulfotransferases which catalyze the addition of sulfate molecules at the 4 and 6 carbons of Gal*N*Ac, and at the 2 and 3 carbons of the GlcA, resulting in various combinations of sulfated GAGs (Kinoshita et al. 2001; Sugahara and Mikami 2007).

Injury to the CNS results in the formation of 'astroglial scar', which prevents severed axons from regenerating (Yiu and He 2006). Although considered a physical barrier to regenerating axons (Reier and Houle 1988), the inhibitory characteristics of astroglial scar were subsequently attributed to the localized increase in expression of CSPGs at the lesion site (McKeon et al. 1991). Further, chondroitinase ABC (chABC) treatment of the glial scar resulted in significant enhancement of neurite outgrowth (Becker and Becker 2002; Bradbury et al. 2002; Lee et al. 2009; McKeon et al. 1995). These results strongly suggest that the inhibitory properties of CSPGs are attributed to the associated CS-GAG chains.

While CS-GAGs contribute to inhibition, the extent of inhibition is dependent on the pattern of CS-GAG sulfation. Sulfated GAGs facilitate specific biological functions such as receptor recognition and subsequent downstream cell signaling (Honke and Taniguchi 2002). Oversulfated CS-GAGs such as CS-2,6S (CS-D), CS-E, IdoA-GalNAc4,6S (CS-H) and CS-3,4S (CS-K) have unique structural epitopes and hence may participate in interactions with protein ligands (Kinoshita et al. 2001). CS-E is a highly sulfated disaccharide consisting of a GlcUAβ1–3GalNAc (4S,6S) (Uyama et al. 2006). The biosynthesis of CS-E begins with the enzymatic addition of a sulfate to position-4 of the GalNAc residue by the C4ST1, and is completed by the final addition of a sulfate to position-6 of the GalNAc($4SO_4$) by GalNAc4S6ST (Habuchi et al. 2002). Therefore, the biosynthesis of CS-E by GalNAc4S6ST is wholly dependent on the primary sulfation of the terminal GalNAc by C4ST1. Due to presence of several CSPGs *in vivo*, the ability to selectively downregulate only sulfotransferases catalyzing the sulfation of inhibitory CS-GAGs makes for an attractive therapeutic alternative.

We previously demonstrated the nerve inhibitory potential of CS-E and its upregulation in astroglial scar when compared to other CS-GAGs. To further elucidate the role of CS-E in nerve inhibition, we examined GalNAc4S6ST mRNA expression after CNS injury, and used *in vitro* assays to investigate the influence of sulfation patterns of CS-GAGs on neuronal inhibition when presented in solution or when immobilized onto a substrate compared to a CSPG (aggrecan) which is inhibitory only when immobilized. Finally we examined whether the selective downregulation of CS-E alone sufficiently attenuates CSPG mediated inhibition.

Materials and Methods

Cortical stab wound injury

All animal procedures were approved by the Institutional Animal Care and Use Committees (IACUC) at Georgia Institute of Technology. Cortical stab wounds were inflicted upon eight

adult male Sprague Dawley rats (Harlan, Indianapolis, IN) using neural probes that were introduced into two 3 mm holes, created 0.2 mm anterior and 3 mm lateral to the bregma according to methods previously published (Zhong and Bellamkonda 2007).

Tissue Preparation for Immunohistochemistry and In situ hybridization

Four weeks after injury, Sprague Dawley rats (Harlan, Indianapolis, IN) inflicted with cortical stab wounds were perfused transcardially with 0.1 M PBS (pH 7.4) followed by 4% paraformaldehyde in 0.1 M PBS (pH 7.4). Brains were dissected out, soaked for 48 h in 30% sucrose made with 0.1 M PBS (pH 7.4) at 4 °C, and finally embedded in Tissue Tek OCT (Sakura Finetek, Torrence, CA) compound and stored at −80 °C until sectioned.

20 µm sections for immunohistochemistry and 7 µm for *in situ* hybridization were prepared in a cryostat and collected. All solutions used for *in situ* hybridization were conducted in 0.1% diethyl pyrocarbonate (DEPC) water to prevent mRNA degradation by RNases. Hybridization was performed according to methods provided by GeneDetect (GeneDetect, Bradenton, FL). Control sections were treated with RNase A (20 mg/ml) at 37 °C for 30 min prior to probe hybridization. Slides incubated in probe containing hybridization buffer were subsequently wrapped in parafilm and incubated overnight in a humidified 37 °C incubator. Post hybridization, the slides were washed twice for 10 min each at 55 °C in 1 X SSC (salinesodium citrate) solution, followed by two washes in 0.5 X SSC. Anti-DIG-alkaline phosphatase antibody (Roche diagnostics, Indianapolis, IN) detection of the DIG labeled oligonucleotide probe was visualized using NBT/BCIP (Roche diagnostics, Indianapolis, IN). The sections were finally rinsed twice in PBS and DAPI stained to visualize nuclei. Slides were ultimately mounted using Prolong Gold (Invitrogen, Carlsbad, CA) and imaged using a Ziess Axioskop 2-plus (Carl Zeiss Inc., Thornwood, NY) upright microscope.

Primary Cortical Neuron Harvest and Cell Culture

Cortical neurons were obtained from embryonic day 18 (E18) rat fetuses (Harlan Laboratories, Indianapolis, IN) according to methods previously described (Cullen et al. 2007). The dissociated cells were pelleted by centrifugation at 1000 g for 3 min and resuspended in neuronal media (neurobasal medium + 2 % B-27 + 250 mM Glutamax). Cells were counted using a hemocytometer and plated onto treated surfaces at a density of 60,000 cells/dish. Plated cells were maintained in a 37 °C incubator under conditions of 5 % CO_2 and 95 % humidity for 48 h.

GAG Biotinylation and Substratum Preparation for Spot and Bonhoeffer Stripe Assays

GAGs were biotinylated using methods previously described (Deepa et al. 2002). Briefly, 5 mg/ml concentrations of the CS-GAGs: CS-A (Sigma-Aldrich, St. Louis, MO), CS-C, D and E (Seikagaku Corp, Tokyo, Japan) as well as dermatan sulphate (DS) (Seikagaku Corp, Tokyo, Japan) were prepared in 0.1 M MES [(2-*N*-morpholino) ethanesulfonic acid] buffer and biotinylated using a 50 mM solution of freshly prepared EZ-Link® Biotin Hydrazide (Thermo Fisher Scientific Inc., Rockford, IL) according to protocols provided. Quantification of moles of biotin per mole of GAG was done using the Pierce® biotin quantitation kit and the protocols therein (Thermo Fisher Scientific Inc., Rockford, IL).

Preparation of 14 mm glass-bottomed Petri-dishes (In Vitro Scientific, Sunnyvale, CA) was done according to methods previously described (Tom et al. 2004) with few modifications. Briefly, surfaces were coated with poly-D-lysine (PDL) (Sigma-Aldrich, St. Louis, MO) and incubated overnight at 37 °C. The next day, the surfaces were rinsed thrice with sterile water and allowed to dry completely. Various concentrations of aggrecan, bovine serum albumin (BSA) and biotinylated CS-GAGs; as well as astrocyte conditioned media (ACM) obtained

as described below mixed with Texas Red (Invitrogen, Carlsbad, CA), were spotted onto the prepared surfaces in 2 µl amounts and allowed to dry.

For Bonhoeffer stripe assays, 40 mm − 0.17 mm thick glass coverslips (Biopechs, Butler, PA) were surface treated with PDL as described above and allowed to air dry. Bonhoeffer silicone matrices (Max Planck Institute, Tubingen, Germany) were fixed securely onto the coverslips and 20 µl of ACM mixed with Texas Red (Invitrogen, Carlsbad, CA) at a final concentration of 0.45 mg/ml was injected into the matrix chamber. The injected volume was gently aspirated into the channels and allowed to incubate at 37 °C for 3 hr. The ACM was subsequently aspirated out of the channels and the matrices were gently lifted off from the coverslip and allowed to dry. After the spots and stripes had dried completely dissociated cortical neurons were plated onto the treated surfaces and cultured as described above.

Soluble CSPG/CS-GAG Assays

For the soluble CSPG/CS-GAG assays, the CSPG-aggrecan and CS-E were reconstituted in neurobasal media and added to dissociated cortical neurons resuspended in neuronal medium in a final volume of 250 µl and at a final concentration of 2.8 mg/ml each. The CSPG/CS-GAG containing cell suspension was plated onto 14 mm glass-bottomed Petri-dishes that were surface treated and cultured as described above.

Astrocyte Cell Culture

Primary astrocytes were dissected and dissociated from postnatal day 1 (P1) rat pups (Harlan, Indianapolis, IN) using methods described earlier (Cullen et al. 2007). For siRNA transfections, confluent cultures that had been passaged at least four times, but not more than seven times were used.

Immunohistochemistry

Neuronal cultures were fixed using 1 X PBS containing 4 % paraformaldehyde and 0.4 M sucrose for 30 minutes at room temperature and subsequently washed multiple times using PBS. Blocking solution (4 % Goat Serum, 0.5 % Triton X-100) prepared in PBS was added and allowed to incubate at room temperature for 1 h. Primary antibodies, MAP-2 (Millipore, Temecula, CA) (1:500) and CS-56 (Sigma-Aldrich, St. Louis, MO) (1:220) were made up in blocking solution were then added and allowed to incubate overnight at 4 °C. This was followed by three washes with PBS followed by 1 h incubations with blocking buffer containing the secondary antibodies- Alexa fluor goat Anti-mouse IgG$_1$ 488 (Invitrogen, Carlsbad, CA) (1:220) against MAP-2, and Alexa fluor goat Anti-mouse IgM 594 (Invitrogen, Carlsbad, CA) (1:220) against CS-56. Immobilized biotinylated GAGs were visualized using Alexa fluor streptavidin 594 (Invitrogen, Carlsbad, CA) (1:220). The culture surfaces were then washed thrice with PBS and stained with 4',6-diamidino-2-phenylindole (DAPI) (Invitrogen, Carlsbad, CA) at room temperature for 10 min. Lastly, the surfaces were affixed with 12 mm glass coverslips (VWR, West Chester, PA) using Prolong gold (Invitrogen, Carlsbad, CA) and imaged as explained below.

The 20µM thick tissue sections prepared as described above were blocked in PBS containing 4% normal goat serum with 0.5% Triton X- 100 for 1h at room temperature and then incubated with 1:1000 rabbit polyclonal anti-glial fibrillary acidic protein (GFAP) (Dako, Carpinteria, CA) against reactive astrocytes, and 1:1000 mouse anti-ED1 (AbD Serotec, Raleigh, NC) for 24h at room temperature in PBS containing 4% goat serum and 0.5% Triton X-100. The primary antibodies were then washed several times in PBS and fluorescently labeled with Alexa fluor goat anti-rabbit IgG1 594 for GFAP, and goat anti-mouse IgG1 488 for EDI (Invitrogen, Carlsbad, CA). Finally DAPI (Invitrogen, Carlsbad, CA) staining was done to visualize nuclei. Sections were profusely washed with PBS and

finally mounted in Fluoromount-G™ (SouthernBiotech, Birmingham, AL) and imaged using a Ziess Axioskop 2-plus (Carl Zeiss Inc., Thornwood, NY) upright microscope.

Image analysis

Neuronal cultures were fixed and stained as described above and imaged under a Ziess Axiovert 200M (Carl Zeiss Inc., Thornwood, NY) motorized inverted microscope attached to a Cooke Sensicam QE (The Cooke Corporation, Romulus, MI) monochrome camera which were controlled using ImagePro 7.0 image acquisition software (Media Cybernetics, Bethesda, MD). Zeiss LD Achroplan 20 X and Plan-Apochromat 63 X 1.4 NA objectives was used to acquire low magnification and high magnification Z-stack Images with 0.5 and 0.2 µM increments respectively.

Quantification of axonal crossing, fasciculation and cell attachment

Neurites were scored for axonal crossing and fasciculation along spot boundaries by applying previously described criterion (Snow et al. 2003). For axonal crossing, processes from cells located within a 40 µM region outside of the CSPG/CS-GAG/ACM spot boundary were counted. Only neurites that were non fasciculated (i.e ≤ 1 µM) and that were not sitting on top of the spot border were scored as "crossing" and depicted as a percentage of axonal crossing. For total cell attachment, only single cells present within a 100 µM region on the inner spot boundary were scored.

For ACM Bonhoeffer stripe assays, axonal crossing was assessed according to the selection criteria described above and depicted as percentage crossing. Total cell attachment was determined by counting the total number of round phase-bright cells present on the ACM and PDL lanes (Snow et al. 1996). A total of ~400 neurons sampled from among three different experimental repeats were used for quantification of cell adhesion, axonal crossing and fasciculation.

Quantification of CSPG/CS-GAG adsorption

To quantify CSPG/CS-GAG adsorption on glass-bottomed Petri dishes, MATLAB (MathWorks, Natick, MA) line profile intensity feature was used. Biotin conjugated aggrecan and CS-GAGs were spotted on poly-D-lysine (PDL) coated surfaces and were allowed to dry at room temperature. The dishes were washed multiple times with PBS and stained using Alexa Fluor Streptavidin 594 (Invitrogen, Carlsbad, CA) (1:220) and cover-slipped as described above. Images were acquired as described above at constant exposure and the raw images were then loaded onto MATLAB. Six points on the spot boundary were specified and approximated using the 'spline' function. Thereafter, MATLAB drew individual lines from the boundary to 100µm into the spot and intensity values were recorded and averaged for the different spot concentrations.

siRNA Transfection

siRNA duplex sequences were designed using si*Design*® Center and obtained from Dharmacon (Thermo Fisher Scientific Inc., Rockford, IL). Four duplex siRNA sequences (Table-1) were obtained for each target [C4ST1 and GalNAc4S6ST] in order to improve knockdown efficiency. siRNA duplexes were transfected into plated rat astrocytes using the Amaxa Nucleofector II system and the rat astrocyte nucleofector kit (Lonza AG, Cologne, Germany) and the protocols therein. Transfection efficiency as determined by siGLO green transfection indicator (Thermo Fisher Scientific Inc., Rockford, IL) was found to be ~85–90 %. Cultured astrocytes were plated in DMEM serum-free media at a density of 350,000 cells/well, in six-well tissue culture treated plates (Corning. Lowell, MA) and maintained in a 37 °C incubator under conditions of 5 % CO_2 and 95 % humidity for 24 h. After 24 h,

media was aspirated out and 1 mL of fresh DMEM serum-free media was added to each of the following controls – a) Untreated astrocytes ; b)TGF-α (10 ng/ml) (Chemicon, Temecula, CA) ; c) TGF-α + 10 nM siCONTROL non-targeting scrambled siRNA pool #2 obtained from Dharmacon (Thermo Fisher Scientific Inc., Rockford, IL). The sulfotransferase mRNA targeting treatments included TGF-α, to which 100 nm concentrations of siRNA duplexes targeting a) C4ST1 alone; b) GalNAc4S6ST alone; and c) C4ST1 + GalNAc4S6ST together were added. Each treatment was conducted in triplicate, and each experiment was conducted three different times using different animal cohorts for statistical significance. Plates containing the treatments were returned to the 37 °C incubator and maintained under conditions mentioned above for 48 h. After 48 h, ACM samples and cell pellets were collected for GAG analysis by HPLC and qRT-PCR respectively.

RNA extraction and qRT-PCR Analysis

Total RNA was extracted from cell pellets obtained from the siRNA knockdown experiments using the Qiagen RNEasy Mini Kit (Qiagen Inc., Valencia, CA). Extracted total RNA was quantified using the Quant-iT RiboGreen RNA Reagent and Kit (Invitrogen, Carlsbad, CA). 2 µg of the total RNA was converted to cDNA using a high capacity cDNA reverse transcription kit (Applied Biosystems Inc., Foster City, CA). PCR primers for C4ST1, (chondroitin 4) sulfotransferase 12 (C4ST2), GalNAc4S6ST and the housekeeping gene hypoxanthine phosphoribosyltransferase 1 (HpRT1) (Table-2) were designed using Primer Express® software (Applied Biosystems Inc., Foster City, CA), and obtained from IDT inc. (Integrated DNA Technologies Inc., Coralville, IA). Primer validation and qRT-PCR using SYBR green mix (Applied Biosystems Inc., Foster City, CA) was conducted on a StepOnePlus real time-PCR machine (Applied Biosystems Inc., Foster City, CA) according to methods previously published (Karathanasis et al. 2009). Fold differences calculated using the comparative C_T method were normalized to control astrocyte sample, tabulated as relative quantities and graphed using SigmaPlot 11 software.

Extraction of GAGs from Astrocyte Conditioned Media

ACM samples were concentrated using 30,000 MWCO Vivaspin-6 spin concentrators (GE healthcare, Piscataway, NJ) and total protein was quantified using a dye-binding calorimetric assay (Bio-Rad, Hercules, CA)(Bradford 1976). After conducting spot assays as described above, GAGs were extracted from the remaining ACM samples according to methods previously described (Deakin and Lyon 2008). Briefly, ACM samples were subjected to proteinase digestion with 1 mg/ml pronase (Sigma-Aldrich, St. Louis, MO) at 37 °C for 1 h. Pronase digested samples were passed through DEAE sephacel columns to remove digested proteins and other contaminants. Briefly, 10 ml blank centrifuge columns (Thermo Fisher Scientific Inc., Rockford, IL) were packed with DEAE sephacel (GE healthcare, Piscataway, NJ), and equilibrated using five volumes of PBS. After column equilibration, pronase digested GAG samples were applied to the column and washed with three volumes of 0.25 M NaCl and 10 mM phosphate buffer, pH 7.4, to remove contaminants. Column bound GAG's were eluted with three volumes of 1.5 M NaCl and 10 mM phosphate buffer, pH 7.4, desalted using PD10 columns (GE healthcare, Piscataway, NJ), and freeze-dried overnight. Lyophilized GAG samples were chondroitinase ABC (chABC) (Sigma-Aldrich, St. Louis, MO) digested overnight at 37 °C, using 5 mU enzyme/ 50 µL of 50 mM Tris + 60 mM sodium acetate buffer, pH 7.5, to release CS disaccharides. Enzyme digested samples were freeze-dried overnight.

2-Aminoacridone (AMAC) re-purification and labeling of CS-disaccharides

AMAC re-purification and labeling of CS-disaccharides was conducted using the methods described by Deakin and Lyon (Deakin and Lyon 2008), followed by additional clean-up of unbound AMAC using methods described elsewhere (Hitchcock et al. 2008).

Reverse-phase HPLC of AMAC labeled CS-disaccharides

CS-disaccharide standards and CS-disaccharides extracted from ACM samples were analyzed in 20 µL volumes, injected onto a Phenomenex Luna C18(2) 4.6 I.D X 250mm RP-HPLC column (Phenomenex, Torrence, CA), using methods as described by Deakin and Lyon (Deakin and Lyon 2008). Prior to sample injection, the column was equilibrated with 0.1 M ammonium acetate (solution-A) for 30 min. Samples were separated on a methanol gradient in the following steps: step 1 – 2 min (0–10%); step 2–50 min (10–50%); step 3–20 min (100%); and step 4- (100−0%). Lastly, the column was equilibrated in solution-A as mentioned above, followed by subsequent sample injection and repetition of the gradient separation. Sample peaks were detected by excitation at 425 nm and emission at 540 nm using a RF-10Axl fluorescence detector (Shimadzu Scientific Instruments, Columbia, MD). Peak selection and generation of calibration curves was conducted using the Shimadzu LCsolution software (Shimadzu Scientific Instruments, Columbia, MD). CS-disaccharides from ACM samples were compared to the standards to identify unknown peaks and to determine CS-GAG concentrations.

Statistical analysis

Plotted data are represented as mean ± standard deviations (SD) of replicates. Values were analyzed by one-way repeated measures ANOVA and the Holm-Sidak post-hoc test was employed for making pairwise comparisons using SigmaPlot 11 software (Systat, San Jose, CA). P-values ≤ 0.05 were considered statistically significant.

Results

GalNAc4S6ST mRNA is upregulated at the site of CNS injury

Cortical stab wounds were induced in adult rats and the tissue was harvested for *in situ* hybridization to qualitatively assess GalNAc4S6ST mRNA expression after injury. The cortical sections processed for *in situ* hybridization were DAPI stained in order to localize the stab wound made obvious by a dense cluster of nuclei (Fig. 1A). Most of cells surrounding the stab wound overexpress GalNAc4S6ST as indicated by the darker NBT/BCIP staining relative to the surrounding tissue, corroborating our previous finding demonstrating upregulation of in CS-E *in vivo* in adult astroglial scar tissue (Gilbert et al. 2005). To assess the composition of glial cells at the wound area, cortical sections were immunofluorescently labeled with glial fibrillary acidic protein (GFAP) – for astrocytes, and ED1 – for microglia. The wound area was clearly defined by a high concentration of ED1 expressing cells, surrounded by a high number of astrocytes expressing GFAP (Fig.1B, individual markers and high/low resolution composite images).

Surface Immobilized and soluble CS-E significantly inhibits rat cortical neurons in vitro

Using an *in vitro* spot assay designed to mimic glial scar (Tom et al. 2004) we tested whether CS-E is a potent inhibitor of axonal growth and cell attachment. Based on our previous finding that the amount of GAG present in the cortex is approximately 1 µg/mg of protein (Gilbert et al. 2005), we assayed axonal crossing, fasciculation and cell attachment of rat E18 cortical neurons cultured on poly-D-Lysine (PDL) coated glass-bottom Petri-dishes. Since CS-GAGs rarely exist in isolation, we attempted to mimic a situation where a combination of relevant GAGs are presented to neurons by spotting with 2 µL amounts of biotinylated DS + CS - A, C and D and separately with DS + CS - C, D and E at a final concentration of 1.4 mg/ml. DS (previously classified as CS-B) was included in combination with CS-GAGs to verify its inhibitory potential if any. Quantification of axonal crossing showed significant differences (P≤ 0.05) between the two groups with the GAG group devoid of CS-E showing significant axonal crossing across the spot boundary and reduced

fasciculation of axons when compared to the GAG treatment that included CS-E (Fig. 2A and Fig 2C). The GAG group containing CS-E in contrast showed a distinct inhibitory boundary with reduced axonal crossing and cell attachment and increased axonal fasciculation when compared to the GAG group devoid of CS-E (Fig. 2B and Fig. 2D).

In dose response assays with various concentrations of surface immobilized aggrecan, CS-A, CS-E and BSA we show that immobilized aggrecan restricts axonal crossing and cell attachment at the spot boundary (Fig. 3A and Fig.3A*) when compared to the CS-A and BSA (Fig. 3B and 3D). Increasing concentrations of the aggrecan/CS-GAG immobilized was represented by a corresponding increase in fluorescence intensity (Supplementary Fig. 1). Dose response studies with immobilized aggrecan shows significantly reduced axonal crossing (Fig. 3E) and cell attachment (Fig. 3F) and significantly increased axonal fasciculation (Fig. 3E) at the highest concentration assayed (2.8 mg/ml) when compared to BSA assayed at the same concentration and lower concentrations of aggrecan. In comparison, CS-A showed no significant differences in axonal fasciculation and cell attachment (Fig. 3B; Fig. 3G and Fig.3H), although, significant differences in axonal crossing were detected with increasing concentrations of immobilized CS-A (Fig. 3G). CS-E however, showed significantly reduced cell attachment (Fig. 3C and Fig. 3J) and significantly increased fasciculation with increasing concentrations of immobilized CS-E in a manner similar to aggrecan. The 100 µm area from the outer edge of the CSPG/GAG gradient inward was chosen on the basis of our observations indicating little to no cell attachment in the case of Aggrecan and CS-E uniformly across all areas of the spots. While the gradient obtained with spot assays is indeed steep, we were able to consistently see a clear zone of inhibition corresponding to ~100 µm with these treatments. Based on these observations, the 100 µm distance was selected as the criteria for comparison and quantification of cell-attachment for CS-GAG and ACM spots.

Previously reported differences in the inhibitory potential of soluble versus immobilized CSPGs and CS-GAGs prompted us to further explore the inhibitory potential of aggrecan and CS-E when presented in the soluble state to cultured E18 cortical neurons. Our results are in accordance with previous observations (Snow et al. 1996) indicating that soluble aggrecan had no detrimental effects on neurite length and showed no significant differences when compared to PDL control (Fig. 4A; Fig. 4C and Fig. 4D). In contrast, soluble CS-E shows a significant reduction in neurite length when compared to aggrecan and PDL control when assayed at a final concentration of 2.8 mg/ml (Fig. 4D). Overall, these results present new evidence to show that immobilized CS-E is inhibitory to cultured rat E18 cortical neurons, and that this inhibitory trait remains constant when CS-E is presented in solution.

siRNA targeting of C4ST1 and GalNAc4S6ST mRNA results in their selective downregulation and differential regulation of other sulfotransferase species

To verify the influence of specific sulfation patterns on neuronal inhibition, we treated TGFα stimulated rat astrocytes with siRNA targeting C4ST1 and GalNAc4S6ST transcripts. Reactive astrocytes obtained from P1 rat brains were transfected with siRNA duplexes specific for C4ST1 and GalNAc4S6ST. qRT-PCR analyses revealed the significant (P≤0.05) increase in expression of GalNAc4S6ST transcripts in TGFα treated astrocytes when compared to the untreated control (Fig. 5). The mRNA expression profile of sulfotransferases in astrocytes treated with scrambled siRNA was similar to that of TGFα treated astrocytes indicating the absence of any non-specific targeting. Treatment of astrocytes with siRNA targeting C4ST1 transcripts resulted in the specific targeting and reduced expression of the C4ST1 transcript without affecting the levels of C4ST2 and GalNAc4S6ST expression (Fig 5). The siRNA targeting of GalNAc4S6ST mRNA also resulted in the selective downregulation of the GalNAc4S6ST transcripts, however this was also accompanied by the significant increase in expression of the C4ST1 transcript. The dual

siRNA targeting of C4ST1 and GalNAc4S6ST transcripts expectedly downregulated the two transcripts of but also resulted in the concomitant significant increase in expression levels of the C4ST2 transcript. These results confirmed the specificity of siRNA targeting of the sulfotransferase transcripts of interest and also revealed that selective targeting of these transcripts can lead to the induced differential regulation of certain other sulfotransferase species.

Sulfated GAG species are upregulated in TGFα treated astrocytes

The effects of TGFα treatment and selective siRNA targeting of sulfotransferase mRNA on the expression of sulfated GAG species was examined by high performance liquid chromatography (HPLC) analysis of 2-aminoacridone (AMAC) labeled CS-disaccharides. CS-disaccharides were obtained and AMAC labeled after chABC digestion of CS-GAGs extracted from CM of untreated, TGFα, C4ST1 siRNA, GalNAc4S6ST siRNA as well as C4ST1 and GalNAc4S6ST siRNA treated astrocytes. HPLC analysis of AMAC labeled CS-disaccharides led to the identification and quantification of 5 CS-disaccharides: Di-2,6S (CS-D), Di-4,6S (CS-E), Di-4S (CS-A), Di-6S (CS-C) and Di-0S (Fig. 6). Treatment of astrocytes with TGFα alone significantly ($P \leq 0.05$) increased CS-E, CS-C and Di-0S expression, while simultaneously reducing CS-A expression when compared to untreated astrocytes. The CS-GAG expression profile of TGFα + scrambled siRNA treated astrocytes did not differ significantly from that of the TGFα only treated astrocytes. In astrocytes treated with TGFα + C4ST1 siRNA, the significant decrease in CS-A expression is also accompanied by the significant decrease in expression of CS-E, CS-C and Di-0s compared to all other treatments. In contrast, in TGFα + GalNAc4S6ST siRNA treated astrocytes, the specific downregulation of CS-E is accompanied by the significant increase in expression of CS-A, CS-C and Di-0S when compared to the TGFα + C4ST1 siRNA treated sample. The CS-GAG profile of the TGFα + dual siRNA treated samples remained similar to the GalNAc4S6ST siRNA treated samples except for the significant increase in expression of Di-0S. These results provide further evidence that although selective siRNA targeting of sulfotransferases can successfully influence downregulation of the corresponding CS-GAGs, this could also lead to compensatory differential regulation of other CS-GAGs.

Downregulation of C4ST1 and GalNAc4S6ST mRNA mitigates neuronal inhibition

In order to reliably discriminate between the inhibitory states of untreated, TGFα and TGFα + siRNA treated astrocytes, the ACM obtained from the different treatments were subjected to functional tests using both spot assays and Bonhoeffer stripe assays with 0.45 mg/ml of concentrated ACM. The gradients of spot assays with ACM containing Texas Red had a mottled appearance when compared to the CSPG/CS-GAG spots presumably due to the process of drying, however this did not seem to affect the inhibitory properties of the gradient.

Spot assays using ACM indicated that the extent of axonal crossing, fasciculation and cell attachment observed with ACM obtained from untreated astrocytes was similar to that observed in the case of the lowest assayed concentrations of Aggrecan and CS-E. TGFα only treated astrocytes significantly ($P < 0.05$) reduced axonal crossing and cell attachment at the spot boundary and increased axonal fasciculation when compared to all other treatments (Fig. 7B; 7B*; 7F and 7G). Spot assays conducted using ACM from astrocytes treated with TGFα + siRNA targeting C4ST1 mRNA (Fig. 7C; 7C*; 7F and 7G) resulted in significant increase in axonal crossing and cell attachment and reduced axonal fasciculation when compared to ACM from TGFα only treated astrocytes but not when compared to untreated and TGFα + GalNAc4S6ST siRNA treated astrocytes. Assays with ACM from astrocytes treated with TGFα + siRNA targeting GalNAc4S6ST mRNA (Fig. 7D and 7D*) individually and together with TGFα + siRNA targeting C4ST1 mRNA (Fig. 7E and 7E*)

resulted in a significant increase in axonal crossing (Fig. 7F) when compared to all other treatments but showed no significant differences in cell attachment (Fig. 7G) and axonal fasciculation (Fig. 7F) when compared against each other.

Consistent with spot assays, results from a choice assay using the Bonhoeffer stripe assay showed that neurons exposed to stripes containing ACM from TGFα only treated astrocytes displayed significantly reduced axonal crossing and cell attachment when compared to all other treatments. (Fig. 8B; 8B*; 8F and 8G). Neurons exposed to stripes containing ACM from astrocytes treated with TGFα + siRNA targeting C4ST1 (Fig.8C and 8C*) and GalNAc4S6ST mRNA (Fig.8D and 8D*) individually showed significantly more axonal crossing and cell attachment when compared to TGFα only treated astrocytes (Fig.8F and 8G) but showed no significant differences in axonal crossing when compared to ACM from untreated astrocytes. ACM from astrocytes treated with TGFα + siRNA targeting C4ST1 and GalNAc4S6ST mRNA together (Fig.8E and 8E*) showed significant increase in axonal crossing when compared to all other treatments, and also showed a significant increase in cell attachment (Fig. 8G) when compared to all other treatments but showed no significant differences when compared to ACM from astrocytes treated with TGFα + siRNA targeting GalNAc4S6ST mRNA (Fig. 8G). Significantly, the data from both spot and Bonhoeffer assays indicate that downregulation of C4ST1 or GalNAc4S6ST mRNAs individually is sufficient to mitigate neuronal inhibition and this effect is further potentiated when the two transcripts are downregulated in combination.

Discussion

CSPGs in astroglial scar inhibit axonal regeneration. Secreted CSPGs such as aggrecan, versican, neurocan and brevican belong to the lectican family and are important constituents of the developing and mature brain (Maeda et al. 2010a; Maeda et al. 2010b; Margolis et al. 1975; Oohira et al. 1988). Sulfated GAGs play key roles in neuronal cell signaling and inhibition. Analysis of sulfated GAGs purified from developing mouse brains revealed that CS-A, CS-C and unsulfated (CS-0) GAGs comprised the most abundant components, while significant amounts of CS-E was observed in the cerebral cortex (Ishii and Maeda 2008). Disaccharide analysis of rat brain and spinal cord CSPGs also revealed that CS-E content increased by 20% only when detergent extracted (Deepa et al. 2006), indicating that CS-E is likely attached to the perineural net (PNN) associated isoforms of neurocan, brevican, aggrecan and versican. Recently, sulfation patterns of CS-disaccharides have been the subject of much scrutiny (Butterfield et al. 2010; Gilbert et al. 2005; Ito et al. 2010; Properzi et al. 2005; Wang et al. 2008). Properzi et al. (2005) reported that the inhibitory properties of proteoglycans upregulated after CNS injury were mediated by CS-C. Subsequently, we reported the upregulation of a more potently inhibitory CS-GAG, CS-E, in cortical scar tissue (Gilbert et al. 2005). More recent evidence demonstrates that CS-A is a negative regulator of axonal growth (Wang et al. 2008). Despite reports suggesting CS-E to be a growth promoting moiety (Clement et al. 1999; Gama et al. 2006; Nadanaka et al. 1998; Tully et al. 2004), here we present new evidence to show that GalNAc4S6ST mRNA is upregulated after injury, that its product CS-E is inhibitory to cultured embryonic rat E18 cortical neuronal growth, and that its inhibitory potential remains constant when presented in the immobilized and soluble states.

In order to qualitatively and quantitatively assess CS-GAG inhibition of neurons, we used a modified spot assay designed to mimic the glial scar (Tom et al. 2004), as it presents neurons with crude CSPG/GAG gradients, and an inhibitory rim with which cultured neurons can interact. Our spots with CS-GAGs appear to have steeper gradients than that observed in the study conducted by Tom et al. We speculate that this may be due to the absence of a protein core associated with the CS-GAGs or biotinylation of CS-GAGs. Our

data indicates that even low concentrations of immobilized CS-E are sufficient to significantly affect axonal crossing. In comparison, CS-A showed significant differences in axonal crossing only at the highest assayed concentration but did not show any significant differences in cell attachment and axonal fasciculation when compared to aggrecan and CS-E. Deepa et al. (2006) show that urea extraction of rat brain tissue reduced CS-A extraction by 6% when compared to saline extraction, but enriched CS-E extraction by 20% along with other brain CSPGs such as aggrecan, indicating that these CSPGs contain CS-E in addition to other CS-GAGs such as CS-0,C and D. Significantly, our spot assays revealed that the presence of CS-A in combination with other GAGs was less inhibitory to neurons than when CS-A was replaced with CS-E. Addition of CS-E to the mixture drastically decreased axonal crossing, increased axonal fasciculation and decreased cell attachment across the spot boundary demonstrating CS-E to be the most inhibitory GAG. Therefore, presence of CS-E is necessary to elicit a significant inhibitory response that is not replicated by the presence of other CS-GAGs.

Currently it is not known whether CS-E inhibits neurite outgrowth from rat E18 cortical neurons when presented in the soluble state. Previous work by Snow et al.(1996) showed that the addition of soluble CSPG to chicken DRG cultures induced a differential response on neurite initiation when DRGs were cultured on laminin or fibronectin coated surfaces. Subsequently, Rolls et al. (2004) reported that the addition of a 6-sulfated disaccharide (CSPG-DS) to PC12 and organotypic hippocampal slice cultures promoted cell viability and neurite outgrowth. In contrast, our data indicates that unlike other CS-GAGs and CSPGs such as aggrecan, CS-E is a significant ($P \leq 0.05$) inhibitor of neurite outgrowth when presented in the soluble state. These results suggest that CS-GAGs in solution may induce differential effects on neurite outgrowth and viability, and that these effects could be concentration, cell type and sulfation dependent.

CSPGs are also thought to induce the activation and temporal regulation of microglia and macrophages via CD44 receptor signaling. Rolls et al. (2008) report that the inhibition of CSPG biosynthesis immediately following spinal cord injury negatively affects the secretion of neuroprotective factors by microglia/macrophages; while in contrast, inhibition of CSPG biosynthesis 2 days post-injury caused increased expression of neuroprotective factors and was essential to promoting functional recovery. These results indicate that CSPGs also temporally regulate the cellular environment following injury. Although speculative, these molecules could also possibly activate and be secreted by other immunocytic cells such as mast cells. Injury to the CNS is known to induce the influx of mast cells in addition to astroglia (Silver et al. 1996). While mast cell derived neurotrophic factors may help the regenerative potential of neurons following CNS injury (Leon et al. 1994), mast cells also have the ability to encapsulate CS-E in their secretory granules (Razin et al. 1984; Razin et al. 1982; Stevens et al. 1988). Mast cells are attracted chemotactically by astrocytic secretions such as TGFβ1 (Gruber et al. 1994; Shalit et al. 1993). Hence injury induced chemotactic accumulation of mast cells and their subsequent degranulation and release of inhibitory CS-E as well as a number of proteases (Silver et al. 1996) may have detrimental effects on nerve regeneration. CS-E or CS-E rich PG's may then possibly bind to members of the diverse family of transmembrane protein tyrosine phosphatase (PTP) family of neuronal cell-surface receptors (Shen et al. 2009) leading to regenerative failure.

When considering a therapeutic strategy to alleviate CSPG mediated inhibition, it may be useful to adopt a minimalist approach that balances alleviation of inhibition and containment of the wound. Approaches such as chondroitinase ABC (chABC) delivery lead to the nonspecific digestion of all CS-GAGs, and also leave behind undigested sugars in the form of 'stubs' that could continue to inhibit neurons. Modulation of inhibitory CS-GAG sulfation represents a subtle but potentially more effective approach towards alleviation of CNS

inhibition. Wang et al., (2008) recently showed that selective downregulation of C4ST1 results in mitigation of CSPG mediated inhibition. CS-A is one of the most abundantly expressed sulfated GAGs in the CNS (Galtrey and Fawcett 2007) and plays an important role in the maintenance of glial boundaries. Hence the downregulation of CS-A may result in disruption of these boundaries and proliferation of unregulated plasticity. Since CS-E results from the GalNAc4S6ST catalyzed 6 carbon sulfation of the 4 sulfated CS-A, and since CS-E is the most potently inhibitory CS-GAG in our *in vitro* assays, we specifically downregulated C4ST1 and GalNAc4S6ST encoding mRNA in TGFα stimulated astrocytes using siRNA duplexes designed to target the individual transcripts.

We used TGFα since it is known to increase expression of long and short isoforms of receptor protein tyrosine phosphatase β (RPTPβ) as well as phosphocan, that blocks the outgrowth promoting effects of laminin via a mechanism that does not involve CS chains (Dobbertin et al. 2003). However, intrathecal administration of TGFα reportedly increased laminin expression leading to increased neurite out growth in a mouse spinal cord contusion injury model (White et al. 2008). While discrepancies in TGFα dosage may have significantly contributed to the observed contrasting results in these studies, it is generally accepted that TGFα increases CSPG expression to a similar extent as TGF-β1 and epidermal growth factor (EGF) (Smith and Strunz 2005).

When astrocytes were treated with TGFα + siRNA targeting C4ST1 mRNA alone, a significant (P≤0.05) downregulation of the C4ST1 transcript occurred without affecting the expression levels of C4ST2 mRNA. Interestingly, we found that in astrocytes treated with TGFα + siRNA targeting GalNAc4S6ST individually and together with C4ST1 siRNA, a significant downregulation of GalNAc4S6ST mRNA was accompanied by a corresponding significant upregulation of C4ST1 mRNA. Additionally, in astrocytes treated with TGFα + siRNA targeting both C4ST1 and GalNAc4S6ST mRNA together, the significant downregulation of both transcripts resulted in the significant upregulation of C4ST2 mRNA. These results indicate that downregulation of sulfotransferase mRNAs may consequently lead to the compensatory differential regulation and expression of other sulfotransferase mRNAs. This differential regulation was present not only at the RNA level but also when we employed a highly sensitive HPLC technique (Deakin and Lyon 2008). While confirming the majority of our qRT-PCR data, composition analysis of ACM derived CS-GAGs revealed interesting variations in expression of other CS-GAGs. For instance, the significant increase in CS-E expression in TGFα only treated astrocytes is consistent with our observations measuring transcript abundance using qRT-PCR, indicating that CS-E may play an important role in potentiating the inhibitory properties of CSPGs. Interestingly however, the reduced expression of CS-A in these samples does not correlate with our observations from qRT-PCR. Additionally, TGFα only treated astrocytes also demonstrated a significant increase in expression of CS-C and unsulfated (Di0S) CS-GAGs along with the significant decrease in expression of CS-D and CS-A. CS-C has been previously reported to be significantly upregulated *in vitro* after treatment with TGFα and *in vivo* after CNS injury (Properzi et al. 2005). Thus the observed increase in CS-C expression upon cytokine stimulation may indicate a possible inhibitory role for this CS-GAG. Overall, our HPLC analyses supported our qRT-PCR results, and confirmed the observation that siRNA mediated modulation of target sulfotransferase mRNA expression not only downregulates the corresponding CS-GAGs but also induces differential regulation of other CS-GAGs possibly as a means of compensating for the loss of individual CS-GAGs. Given that multiple families of CS-GAG chains are linked to CSPGs, the cumulative contribution of relevant GAGs to neuronal inhibition is entirely plausible. Hence, although siRNA mediated downregulation of relevant inhibitory CS-GAGs offers an attractive therapeutic avenue, the biological consequences of siRNA induced compensatory regulation of sulfotransferase mRNA and CS-GAGs are unknown and need to be investigated further.

In order to assess the functional effects of siRNA targeting, we assayed the inhibitory potential of ACM obtained from untreated, TGFα, TGFα + C4ST1 siRNA, TGFα + GalNAc4S6ST siRNA and TGFα + C4ST1 and GalNAc4S6ST siRNA treated astrocytes on rat E18 cortical neurons. Downregulation of C4ST1 and GalNAc4S6ST mRNA either individually or together, significantly mitigated the inhibitory effects of TGFα treatment. The observed reduction in neuronal inhibition associated with C4ST1 downregulation is likely due to the consequent downregulation of CS-E expression (as confirmed by HPLC), and possibly explains why Wang et al.(2008) observed reduced inhibition in their experiments targeting C4ST1.

In summary, our findings demonstrate: 1) the increased expression of GalNAc4S6ST mRNA at the site of CNS injury *in vivo*; 2) the presence or absence of CS-E significantly alters the inhibitory potential when a mixture of relevant GAGs are presented to cortical neurons; 3) Unlike other CS-GAGs and CSPGs, CS-E is potent inhibitor of rat E18 cortical neurons when substrate immobilized as well as when presented in solution; 4) targeted siRNA mediated downregulation of GalNAc4S6ST mRNA and consequent downregulation of CS-E alone significantly alleviates CSPG mediated inhibition of rat E18 cortical neurons.

Supplementary Material

Refer to Web version on PubMed Central for supplementary material.

Acknowledgments

References

Baker JR, Roden L, Stoolmiller AC. Biosynthesis of chondroitin sulfate proteoglycan. Xylosyl transfer to Smith-degraded cartilage proteoglycan and other exogenous acceptors. J Biol Chem. 1972; 247(12):3838–3847. [PubMed: 4338229]

Becker CG, Becker T. Repellent guidance of regenerating optic axons by chondroitin sulfate glycosaminoglycans in zebrafish. J Neurosci. 2002; 22(3):842–853. [PubMed: 11826114]

Bradbury EJ, Moon LD, Popat RJ, King VR, Bennett GS, Patel PN, Fawcett JW, McMahon SB. Chondroitinase ABC promotes functional recovery after spinal cord injury. Nature. 2002; 416(6881):636–640. [PubMed: 11948352]

Bradford MM. A rapid and sensitive method for the quantitation of microgram quantities of protein utilizing the principle of protein-dye binding. Anal Biochem. 1976; 72:248–254. [PubMed: 942051]

Butterfield KC, Conovaloff A, Caplan M, Panitch A. Chondroitin sulfate-binding peptides block chondroitin 6-sulfate inhibition of cortical neurite growth. Neurosci Lett. 2010; 478(2):82–87. [PubMed: 20450957]

Clement AM, Sugahara K, Faissner A. Chondroitin sulfate E promotes neurite outgrowth of rat embryonic day 18 hippocampal neurons. Neurosci Lett. 1999; 269(3):125–128. [PubMed: 10454148]

Cullen DK, Stabenfeldt SE, Simon CM, Tate CC, LaPlaca MC. In vitro neural injury model for optimization of tissue-engineered constructs. J Neurosci Res. 2007; 85(16):3642–3651. [PubMed: 17671988]

Deakin JA, Lyon M. A simplified and sensitive fluorescent method for disaccharide analysis of both heparan sulfate and chondroitin/dermatan sulfates from biological samples. Glycobiology. 2008; 18(6):483–491. [PubMed: 18378523]

Deepa SS, Carulli D, Galtrey C, Rhodes K, Fukuda J, Mikami T, Sugahara K, Fawcett JW. Composition of perineuronal net extracellular matrix in rat brain: a different disaccharide

composition for the net-associated proteoglycans. J Biol Chem. 2006; 281(26):17789–17800. [PubMed: 16644727]

Deepa SS, Umehara Y, Higashiyama S, Itoh N, Sugahara K. Specific molecular interactions of oversulfated chondroitin sulfate E with various heparin-binding growth factors. Implications as a physiological binding partner in the brain and other tissues. J Biol Chem. 2002; 277(46):43707–43716. [PubMed: 12221095]

Dobbertin A, Rhodes KE, Garwood J, Properzi F, Heck N, Rogers JH, Fawcett JW, Faissner A. Regulation of RPTPbeta/phosphacan expression and glycosaminoglycan epitopes in injured brain and cytokine-treated glia. Mol Cell Neurosci. 2003; 24(4):951–971. [PubMed: 14697661]

Galtrey CM, Fawcett JW. The role of chondroitin sulfate proteoglycans in regeneration and plasticity in the central nervous system. Brain Res Rev. 2007; 54(1):1–18. [PubMed: 17222456]

Gama CI, Tully SE, Sotogaku N, Clark PM, Rawat M, Vaidehi N, Goddard WA 3rd, Nishi A, Hsieh-Wilson LC. Sulfation patterns of glycosaminoglycans encode molecular recognition and activity. Nat Chem Biol. 2006; 2(9):467–473. [PubMed: 16878128]

Gilbert RJ, McKeon RJ, Darr A, Calabro A, Hascall VC, Bellamkonda RV. CS-4,6 is differentially upregulated in glial scar and is a potent inhibitor of neurite extension. Mol Cell Neurosci. 2005; 29(4):545–558. [PubMed: 15936953]

Grimpe B, Silver J. The extracellular matrix in axon regeneration. Prog Brain Res. 2002; 137:333–349. [PubMed: 12440376]

Gruber BL, Marchese MJ, Kew RR. Transforming growth factor-beta 1 mediates mast cell chemotaxis. J Immunol. 1994; 152(12):5860–5867. [PubMed: 7515916]

Habuchi O, Moroi R, Ohtake S. Enzymatic synthesis of chondroitin sulfate E by N-acetylgalactosamine 4-sulfate 6-O-sulfotransferase purified from squid cartilage. Anal Biochem. 2002; 310(2):129–136. [PubMed: 12423630]

Helting T, Roden L. Biosynthesis of chondroitin sulfate. I. Galactosyl transfer in the formation of the carbohydrate-protein linkage region. J Biol Chem. 1969a; 244(10):2790–2798. [PubMed: 5770002]

Helting T, Roden L. Biosynthesis of chondroitin sulfate. II. Glucuronosyl transfer in the formation of the carbohydrate-protein linkage region. J Biol Chem. 1969b; 244(10):2799–2805. [PubMed: 5770003]

Hitchcock AM, Bowman MJ, Staples GO, Zaia J. Improved workup for glycosaminoglycan disaccharide analysis using CE with LIF detection. Electrophoresis. 2008; 29(22):4538–4548. [PubMed: 19035406]

Honke K, Taniguchi N. Sulfotransferases and sulfated oligosaccharides. Med Res Rev. 2002; 22(6):637–654. [PubMed: 12369092]

Ishii M, Maeda N. Oversulfated chondroitin sulfate plays critical roles in the neuronal migration in the cerebral cortex. J Biol Chem. 2008; 283(47):32610–32620. [PubMed: 18819920]

Ito Z, Sakamoto K, Imagama S, Matsuyama Y, Zhang H, Hirano K, Ando K, Yamashita T, Ishiguro N, Kadomatsu K. N-acetylglucosamine 6-O-sulfotransferase-1-deficient mice show better functional recovery after spinal cord injury. J Neurosci. 2010; 30(17):5937–5947. [PubMed: 20427653]

Karathanasis E, Chan L, Karumbaiah L, McNeeley K, D'Orsi CJ, Annapragada AV, Sechopoulos I, Bellamkonda RV. Tumor vascular permeability to a nanoprobe correlates to tumor-specific expression levels of angiogenic markers. PLoS One. 2009; 4(6):e5843. [PubMed: 19513111]

Kinoshita A, Yamada S, Haslam SM, Morris HR, Dell A, Sugahara K. Isolation and structural determination of novel sulfated hexasaccharides from squid cartilage chondroitin sulfate E that exhibits neuroregulatory activities. Biochemistry. 2001; 40(42):12654–12665. [PubMed: 11601990]

Lamberg SI, Stoolmiller AC. Glycosaminoglycans. A biochemical and clinical review. J Invest Dermatol. 1974; 63(6):433–449. [PubMed: 4139221]

Lee H, McKeon RJ, Bellamkonda RV. Sustained delivery of thermostabilized chABC enhances axonal sprouting and functional recovery after spinal cord injury. Proc Natl Acad Sci U S A. 2009; 107(8):3340–3345. [PubMed: 19884507]

Leon A, Buriani A, Dal Toso R, Fabris M, Romanello S, Aloe L, Levi-Montalcini R. Mast cells synthesize, store, and release nerve growth factor. Proc Natl Acad Sci U S A. 1994; 91(9):3739–3743. [PubMed: 8170980]

Maeda N, Fukazawa N, Ishii M. Chondroitin sulfate proteoglycans in neural development and plasticity. Front Biosci. 2010a; 15:626–644. [PubMed: 20036837]

Maeda N, Ishii M, Nishimura K, Kamimura K. Functions of Chondroitin Sulfate and Heparan Sulfate in the Developing Brain. Neurochem Res. 2010b

Margolis RU, Margolis RK, Chang LB, Preti C. Glycosaminoglycans of brain during development. Biochemistry. 1975; 14(1):85–88. [PubMed: 122810]

Matthews RT, Kelly GM, Zerillo CA, Gray G, Tiemeyer M, Hockfield S. Aggrecan glycoforms contribute to the molecular heterogeneity of perineuronal nets. J Neurosci. 2002; 22(17):7536–7547. [PubMed: 12196577]

McKeon RJ, Hoke A, Silver J. Injury-induced proteoglycans inhibit the potential for laminin-mediated axon growth on astrocytic scars. Exp Neurol. 1995; 136(1):32–43. [PubMed: 7589332]

McKeon RJ, Schreiber RC, Rudge JS, Silver J. Reduction of neurite outgrowth in a model of glial scarring following CNS injury is correlated with the expression of inhibitory molecules on reactive astrocytes. J Neurosci. 1991; 11(11):3398–3411. [PubMed: 1719160]

Nadanaka S, Clement A, Masayama K, Faissner A, Sugahara K. Characteristic hexasaccharide sequences in octasaccharides derived from shark cartilage chondroitin sulfate D with a neurite outgrowth promoting activity. J Biol Chem. 1998; 273(6):3296–3307. [PubMed: 9452446]

Oohira A, Matsui F, Matsuda M, Takida Y, Kuboki Y. Occurrence of three distinct molecular species of chondroitin sulfate proteoglycan in the developing rat brain. J Biol Chem. 1988; 263(21):10240–10246. [PubMed: 3392012]

Properzi F, Carulli D, Asher RA, Muir E, Camargo LM, van Kuppevelt TH, ten Dam GB, Furukawa Y, Mikami T, Sugahara K, et al. Chondroitin 6-sulphate synthesis is up-regulated in injured CNS, induced by injury-related cytokines and enhanced in axon-growth inhibitory glia. Eur J Neurosci. 2005; 21(2):378–390. [PubMed: 15673437]

Razin E, Ihle JN, Seldin D, Mencia-Huerta JM, Katz HR, LeBlanc PA, Hein A, Caulfield JP, Austen KF, Stevens RL. Interleukin 3: A differentiation and growth factor for the mouse mast cell that contains chondroitin sulfate E proteoglycan. J Immunol. 1984; 132(3):1479–1486. [PubMed: 6198393]

Razin E, Stevens RL, Akiyama F, Schmid K, Austen KF. Culture from mouse bone marrow of a subclass of mast cells possessing a distinct chondroitin sulfate proteoglycan with glycosaminoglycans rich in N-acetylgalactosamine-4,6-disulfate. J Biol Chem. 1982; 257(12):7229–7236. [PubMed: 6806269]

Reier PJ, Houle JD. The glial scar: its bearing on axonal elongation and transplantation approaches to CNS repair. Adv Neurol. 1988; 47:87–138. [PubMed: 3278533]

Rohrmann K, Niemann R, Buddecke E. Two N-acetylgalactosaminyltransferase are involved in the biosynthesis of chondroitin sulfate. Eur J Biochem. 1985; 148(3):463–469. [PubMed: 3922754]

Rolls A, Avidan H, Cahalon L, Schori H, Bakalash S, Litvak V, Lev S, Lider O, Schwartz M. A disaccharide derived from chondroitin sulphate proteoglycan promotes central nervous system repair in rats and mice. Eur J Neurosci. 2004; 20(8):1973–1983. [PubMed: 15450076]

Rolls A, Shechter R, London A, Segev Y, Jacob-Hirsch J, Amariglio N, Rechavi G, Schwartz M. Two faces of chondroitin sulfate proteoglycan in spinal cord repair: a role in microglia/macrophage activation. PLoS Med. 2008; 5(8):e171. [PubMed: 18715114]

Schwartz NB, Roden L. Biosynthesis of chondroitin sulfate. Purification of UDP-D-xylose:core protein beta-D-xylosyltransferase by affinity chromatography. Carbohydr Res. 1974; 37(1):167–180. [PubMed: 4214614]

Schwartz NB, Roden L. Biosynthesis of chondroitin sulfate. Solubilization of chondroitin sulfate glycosyltransferases and partial purification of uridine diphosphate-D-galactose:D-xylose galactosyltrans. J Biol Chem. 1975; 250(13):5200–5207. [PubMed: 1150655]

Schwartz NB, Roden L, Dorfman A. Biosynthesis of chondroitin sulfate: interaction between xylosyltransferase and galactosyltransferase. Biochem Biophys Res Commun. 1974; 56(3):717–724. [PubMed: 4857056]

Shalit M, Brenner T, Shohami E, Levi-Schaffer F. Interaction between mast cells and glial cells: an in vitro study. J Neuroimmunol. 1993; 43(1–2):195–199. [PubMed: 7681449]

Shen Y, Tenney AP, Busch SA, Horn KP, Cuascut FX, Liu K, He Z, Silver J, Flanagan JG. PTPsigma is a receptor for chondroitin sulfate proteoglycan, an inhibitor of neural regeneration. Science. 2009; 326(5952):592–596. [PubMed: 19833921]

Silver R, Silverman AJ, Vitkovic L, Lederhendler II. Mast cells in the brain: evidence and functional significance. Trends Neurosci. 1996; 19(1):25–31. [PubMed: 8787137]

Smith GM, Strunz C. Growth factor and cytokine regulation of chondroitin sulfate proteoglycans by astrocytes. Glia. 2005; 52(3):209–218. [PubMed: 15968632]

Snow DM, Brown EM, Letourneau PC. Growth cone behavior in the presence of soluble chondroitin sulfate proteoglycan (CSPG), compared to behavior on CSPG bound to laminin or fibronectin. Int J Dev Neurosci. 1996; 14(3):331–349. [PubMed: 8842808]

Snow DM, Smith JD, Cunningham AT, McFarlin J, Goshorn EC. Neurite elongation on chondroitin sulfate proteoglycans is characterized by axonal fasciculation. Exp Neurol. 2003; 182(2):310–321. [PubMed: 12895442]

Snow DM, Steindler DA, Silver J. Molecular and cellular characterization of the glial roof plate of the spinal cord and optic tectum: a possible role for a proteoglycan in the development of an axon barrier. Dev Biol. 1990; 138(2):359–376. [PubMed: 1690673]

Stevens RL, Fox CC, Lichtenstein LM, Austen KF. Identification of chondroitin sulfate E proteoglycans and heparin proteoglycans in the secretory granules of human lung mast cells. Proc Natl Acad Sci U S A. 1988; 85(7):2284–2287. [PubMed: 3353378]

Stoolmiller AC, Horwitz AL, Dorfman A. Biosynthesis of the chondroitin sulfate proteoglycan. Purification and properties of xylosyltransferase. J Biol Chem. 1972; 247(11):3525–3532. [PubMed: 5030630]

Sugahara K, Mikami T. Chondroitin/dermatan sulfate in the central nervous system. Curr Opin Struct Biol. 2007; 17(5):536–545. [PubMed: 17928217]

Tom VJ, Steinmetz MP, Miller JH, Doller CM, Silver J. Studies on the development and behavior of the dystrophic growth cone, the hallmark of regeneration failure, in an in vitro model of the glial scar and after spinal cord injury. J Neurosci. 2004; 24(29):6531–6539. [PubMed: 15269264]

Tully SE, Mabon R, Gama CI, Tsai SM, Liu X, Hsieh-Wilson LC. A chondroitin sulfate small molecule that stimulates neuronal growth. J Am Chem Soc. 2004; 126(25):7736–7737. [PubMed: 15212495]

Uyama T, Ishida M, Izumikawa T, Trybala E, Tufaro F, Bergstrom T, Sugahara K, Kitagawa H. Chondroitin 4-O-sulfotransferase-1 regulates E disaccharide expression of chondroitin sulfate required for herpes simplex virus infectivity. J Biol Chem. 2006; 281(50):38668–38674. [PubMed: 17040900]

Wang H, Katagiri Y, McCann TE, Unsworth E, Goldsmith P, Yu ZX, Tan F, Santiago L, Mills EM, Wang Y, et al. Chondroitin-4-sulfation negatively regulates axonal guidance and growth. J Cell Sci. 2008; 121(Pt 18):3083–3091. [PubMed: 18768934]

White RE, Yin FQ, Jakeman LB. TGF-alpha increases astrocyte invasion and promotes axonal growth into the lesion following spinal cord injury in mice. Exp Neurol. 2008; 214(1):10–24. [PubMed: 18647603]

Yiu G, He Z. Glial inhibition of CNS axon regeneration. Nat Rev Neurosci. 2006; 7(8):617–627. [PubMed: 16858390]

Zhong Y, Bellamkonda RV. Dexamethasone-coated neural probes elicit attenuated inflammatory response and neuronal loss compared to uncoated neural probes. Brain Res. 2007; 1148:15–27. [PubMed: 17376408]
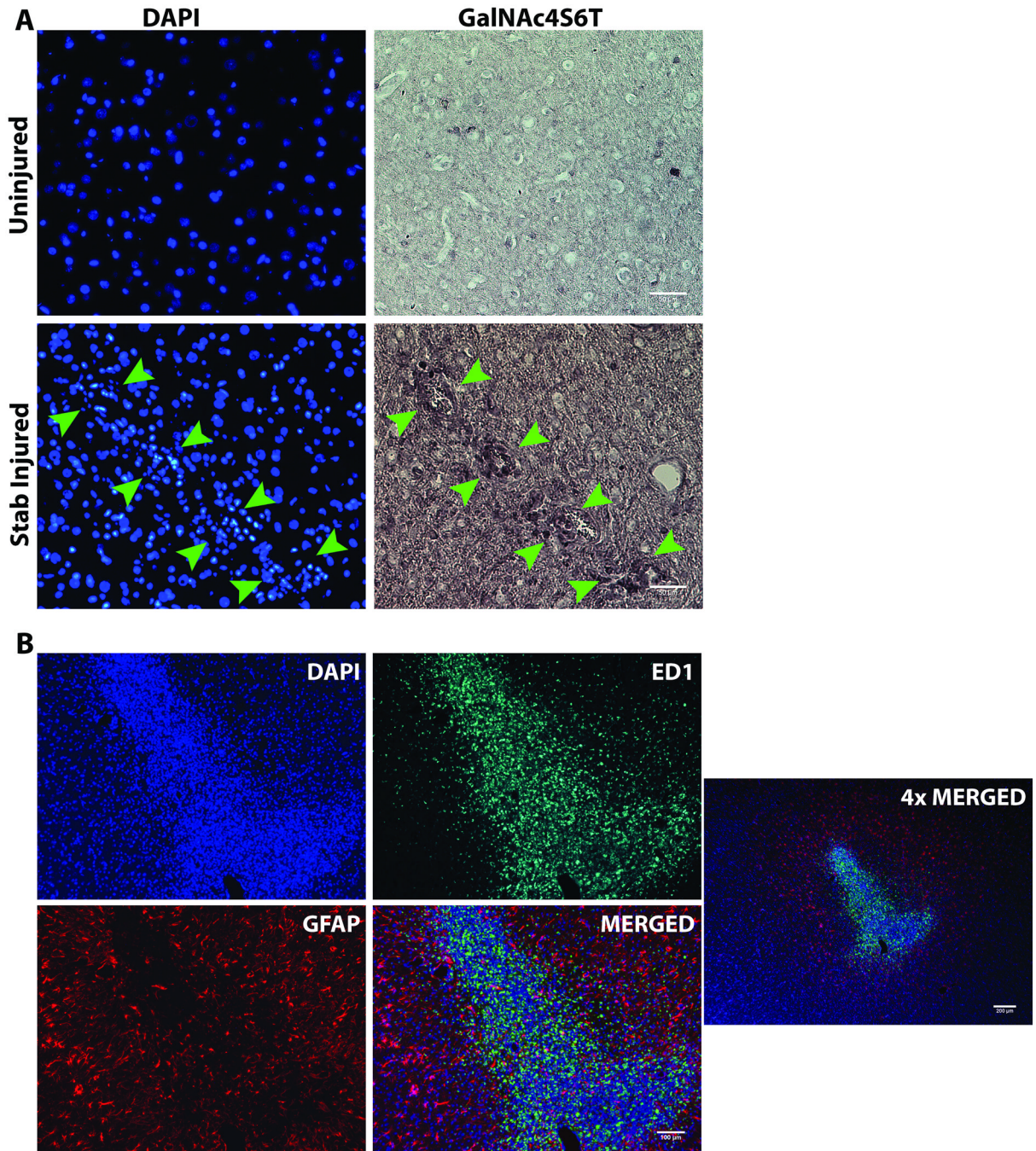
Fig.1.
(A) *In situ* hybridization showing GalNAc4S6ST mRNA upregulation at the site of CNS injury. Uninjured cortex and cortical stab wound site (indicated by green arrow heads) showing DAPI staining and GalNAc4S6ST expression. (B) Immunohistochemical detection of astrocytes (GFAP) and microglia (ED1) at the stab injury site in 20 µm cortical sections. Scale bar = 50 µm, 100 µm and 200 µm respectively.
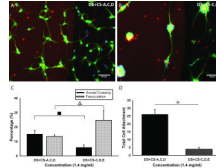
Fig.2.
Combined CS-GAGs containing CS-E inhibits rat E18 cortical neurons. Glass bottom Petri-dishes spotted with 2 µl of 1.4 mg/ml combined CS-GAGs containing A) DS+CS-A,C,D and ; B) DS+CS-C,D,E; C) The DS+CS-C,D and E treatment shows significantly less axonal crossing (■) and increased axonal fasciculation (△) when compared to the DS+CS-A,C and D treatment; D) The DS+CS-C,D and E treatment shows significantly less cell attachment at the spot boundary (*) when compared to the DS+CS-A,C and D treatment. Statistical significance was represented by a P ≤ 0.05; Scale bar = 50 µm.
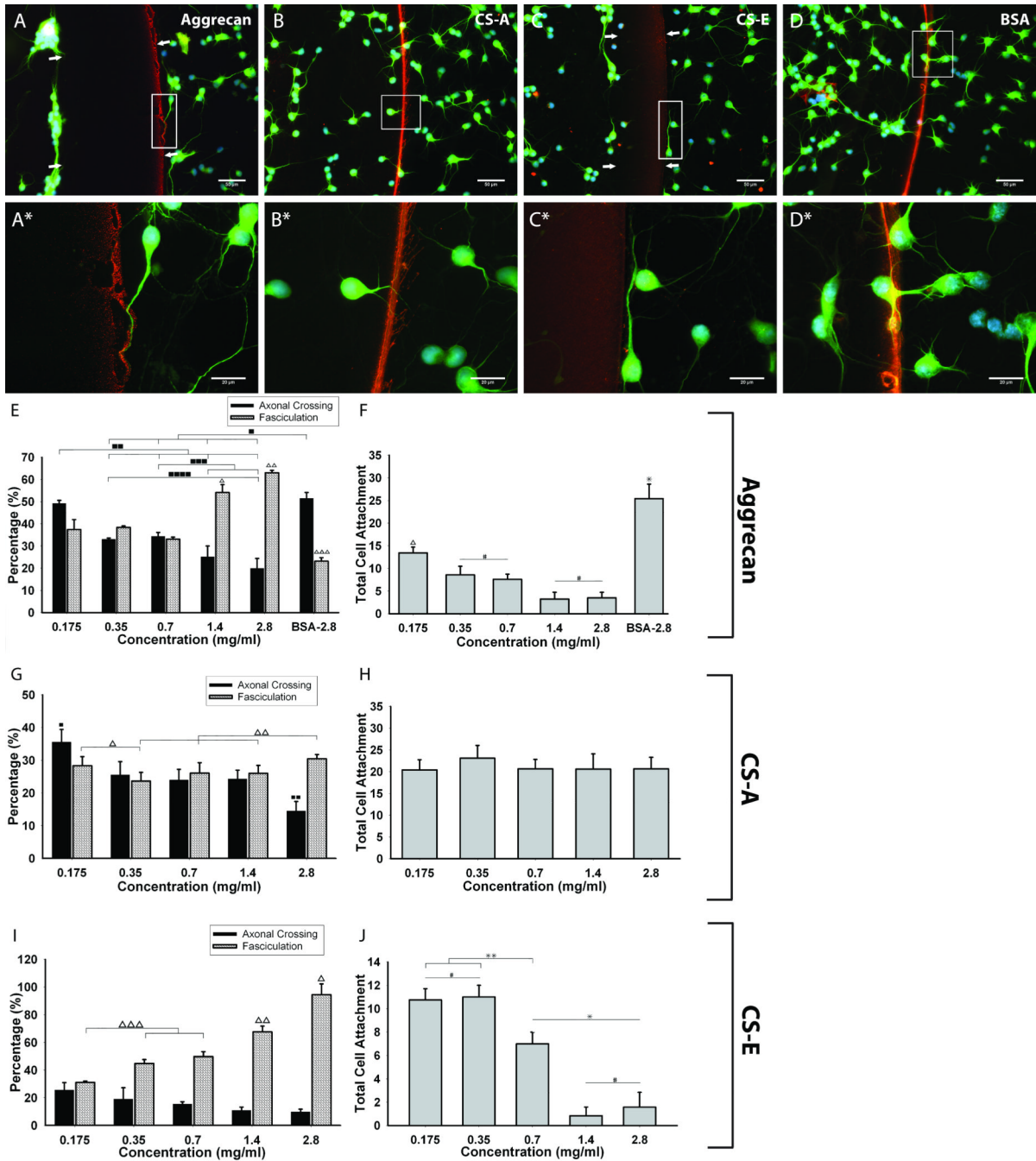
Fig.3.
Aggrecan and CS-E inhibit rat E18 cortical neurons. Glass-bottom Petri-dishes spotted with 2 µl of 1.4 mg/ml A) aggrecan B) CS-A, C) CS-E, and D) BSA. White arrows marking the inhibitory spot borders are represented in A) aggrecan and C) CS-E. High magnification images of boxed regions are presented for A*) aggrecan B*) CS-A, C*) CS-E, and D*) BSA ; E), G) and I) show quantification of axonal crossing and fasciculation across different aggrecan, CS-A and CS-E spot concentrations respectively; F), H) and J) show quantification of cell attachment across different aggrecan, CS-A and CS-E spot concentrations respectively. Statistical significance between treatments is denoted by: ■, ∆,

* and # identifiers and indicate P ≤ 0.05; Scale bar = 50 µm for low magnification and 20 µm for high magnification images respectively.
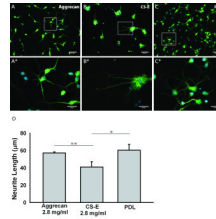
Fig. 4.
CS-E inhibits rat E18 cortical neurons when presented in the soluble state. Glass-bottom Petri-dishes plated with cortical neurons and media containing A) aggrecan B) CS-E at a final concentration of 2.8 mg/ml. Cortical neurons cultured on PDL only treated plates is presented in C). High magnification images of boxed regions are presented for A*) aggrecan B*) CS-E, C*) PDL control. Quantification of neurite length is presented in D) and statistical significance represented by a $P \leq 0.05$ is denoted by * identifiers; Scale bar = 50 µm for low magnification and 20 µm for high magnification images respectively.
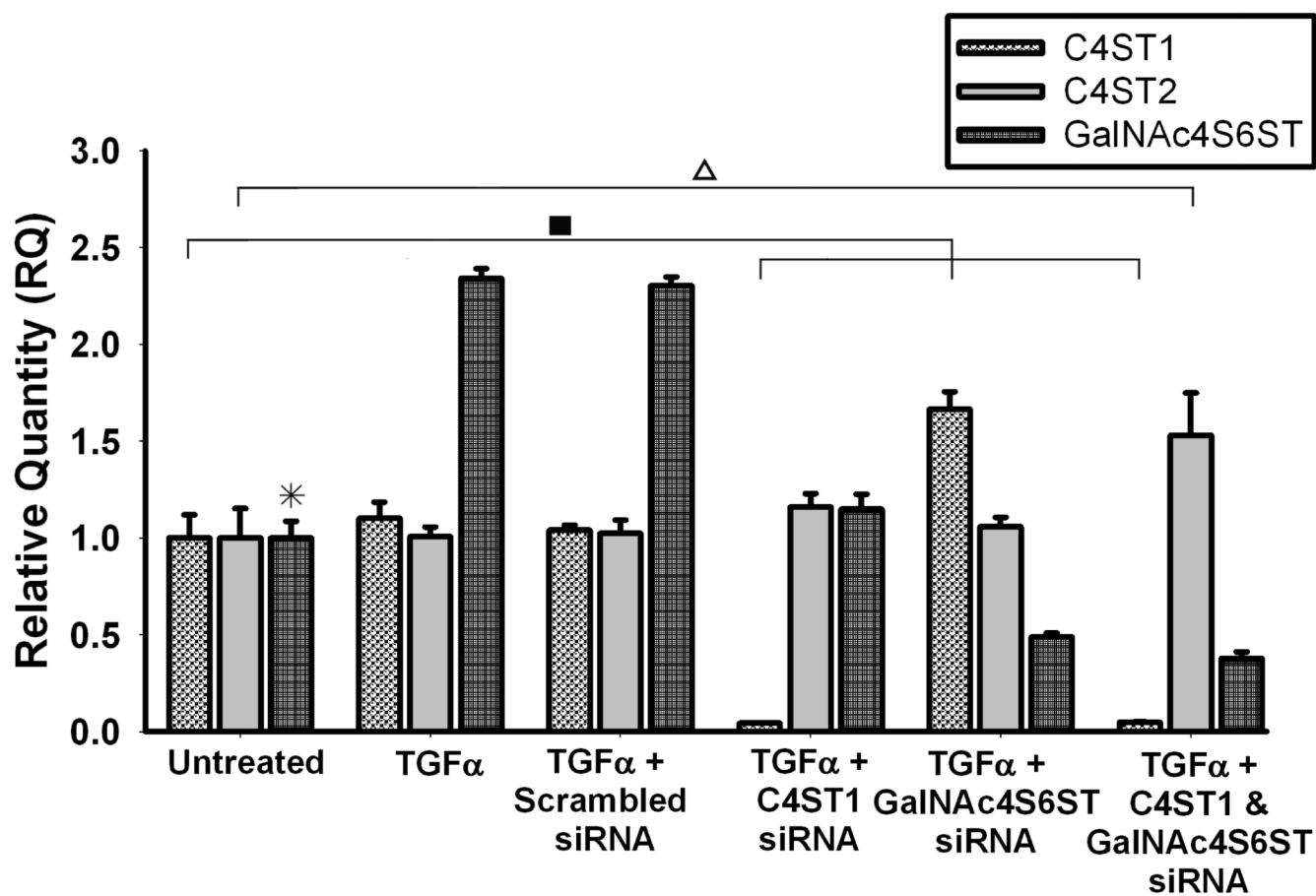
Fig. 5.
TGFα treatment of rat astrocytes significantly upregulates GalNAc4S6ST expression.
Statistical significance between treatments are represented by P ≤ 0.05 and denoted by *, ■
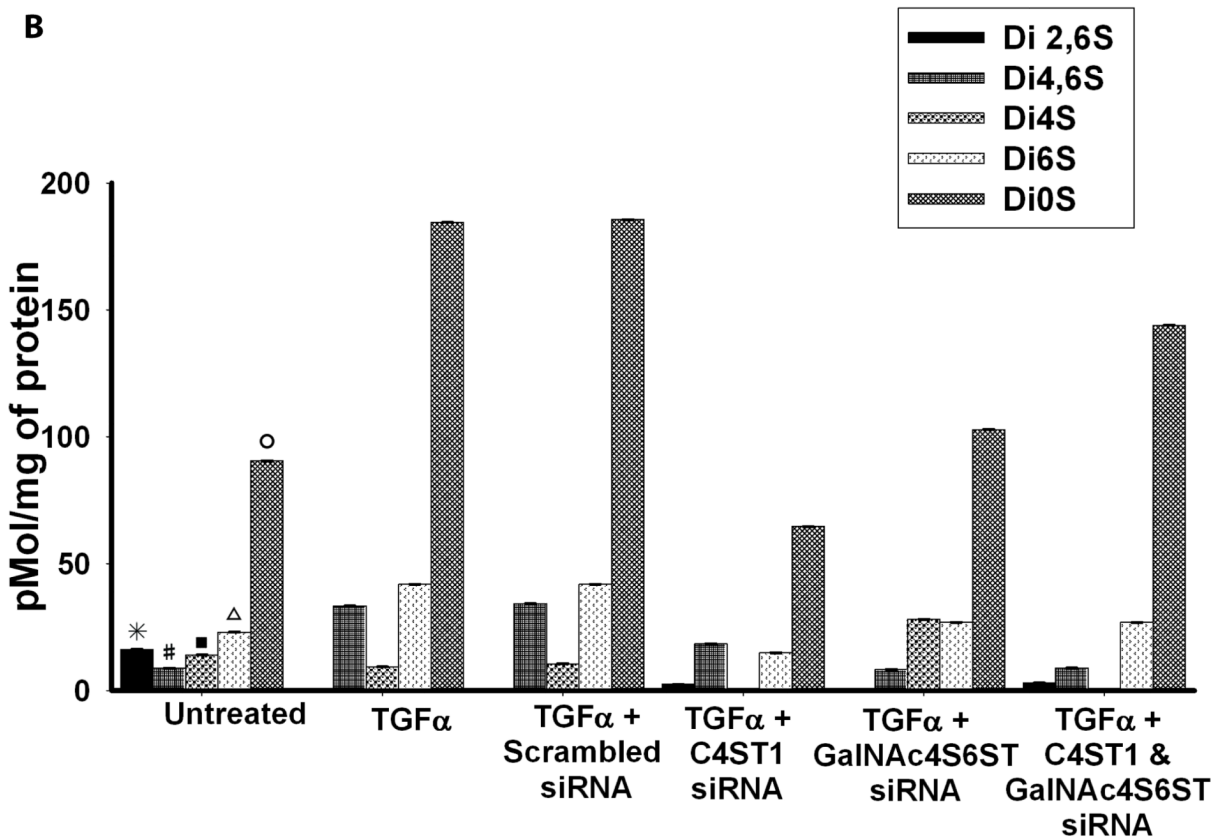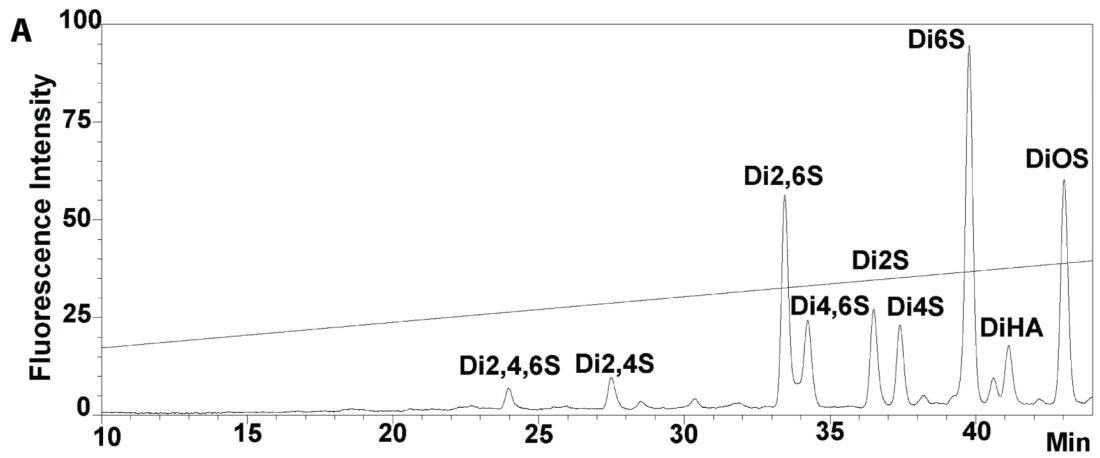and △ identifiers.

Fig. 6.
A) AMAC labeled CS-GAG standards resolved using RP-HPLC B) Composition analysis of CS-GAGs extracted from Untreated, TGFα, TGFα + scrambled siRNA, TGFα + C4ST1 siRNA, TGFα + GalNAc4S6ST siRNA and TGFα + C4ST1 & GalNAc4S6ST siRNA treated astrocytes represented in pMol / mg of protein. Statistical significance is represented by $P \leq 0.05$ and denoted by: *, #, ■, △ and ○ identifiers.
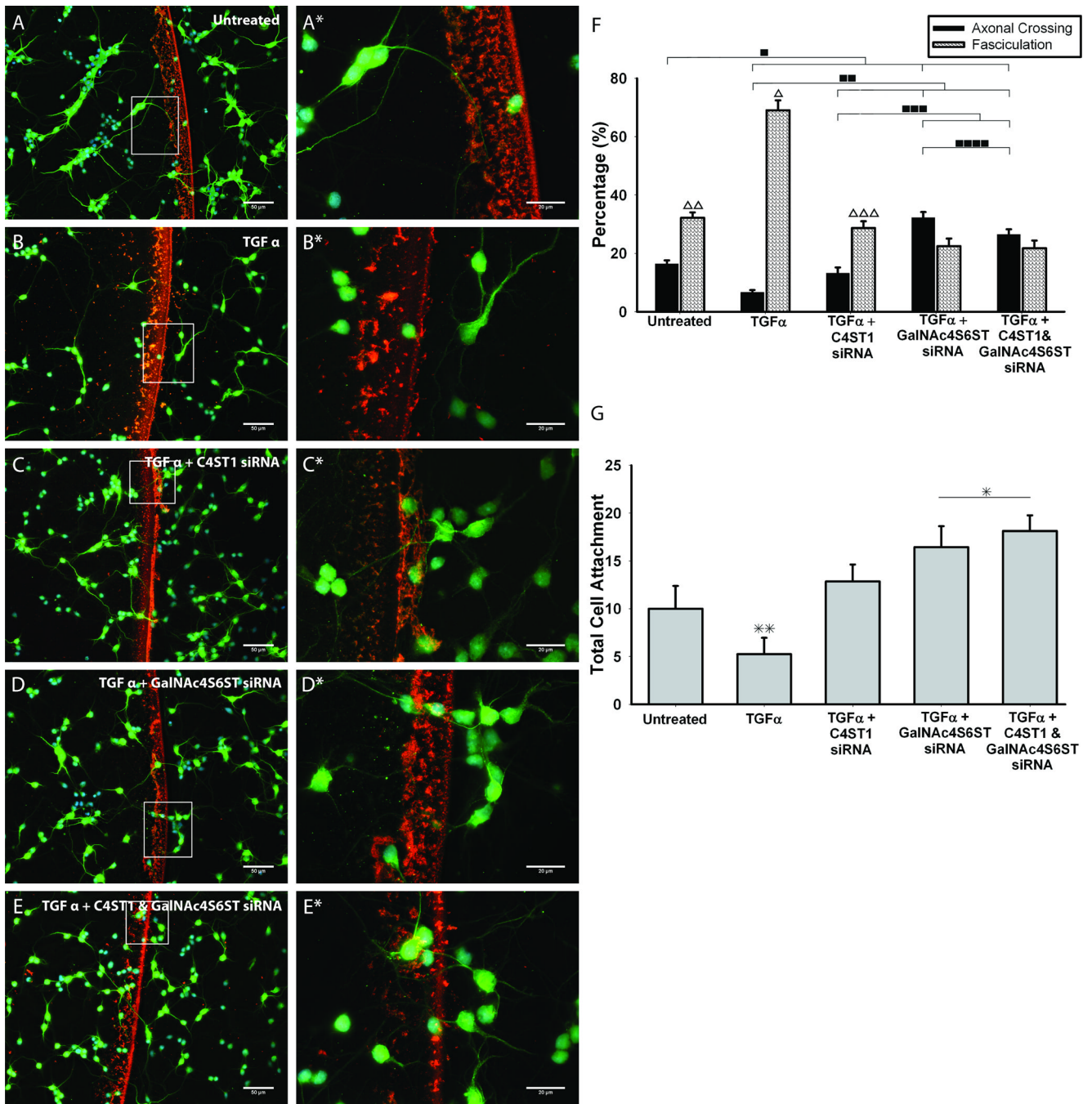
Fig.7.
Spot assays showing treatment of astrocytes with TGFα + siRNA targeting C4ST1 or
GalNAc4S6ST alone or together significantly reduces inhibition. Spot assays were
conducted with 0.45 mg/ml of concentrated ACM from A) control untreated, B) TGFα, C)
TGFα + siRNA against C4ST1, D) TGFα + siRNA against GalNAc4S6ST and E) TGFα +
siRNA against C4ST1 & GalNAc4S6ST together; F) and G) show quantification of axonal
crossing and fasciculation and cell attachment respectively across the different treatments.
Statistical significance is represented by P ≤ 0.05 and denoted by: ■, △, * identifiers; Scale
bar = 50 µm for low magnification and 20 µm for high magnification images respectively.
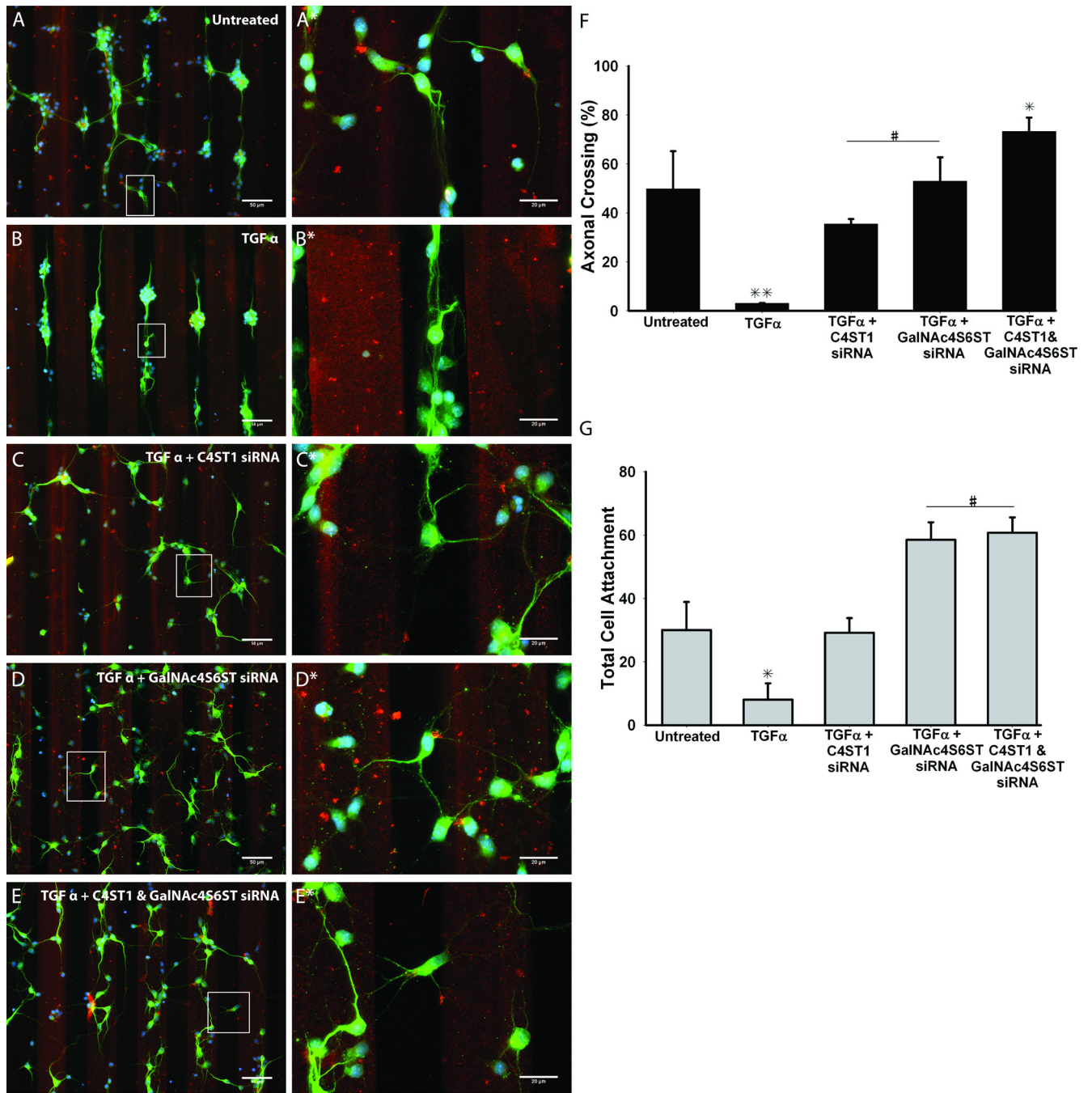
Fig.8.

Bonhoeffer stripe assays showing treatment of astrocytes with TGFα + siRNA targeting C4ST1 or GalNAc4S6ST alone or together significantly reduces inhibition. Stripe assays were conducted with 0.45 mg/ml of concentrated ACM from A) control untreated, B) TGFα, C) TGFα + siRNA against C4ST1, D) TGFα + siRNA against GalNAc4S6ST and E) TGFα + siRNA against C4ST1 & GalNAc4S6ST together. F) and G) show quantification of axonal crossing and cell attachment respectively across the different treatments. Statistical significance is represented by P ≤ 0.05 and denoted by: * and # identifiers; Scale bar = 50 µm for low magnification and 20 µm for high magnification images respectively.

Table – 1

siRNA duplexes

	Sense	Antisense
C4ST1 (Chst11) (NM_001108079.1)	GCAAAGUCCACCCGAACUAUU	5′P UAGUUCGGGUGGACUUUGCUU
	GGGACGAUGUCAAGUUCGAUU	5′P UCGAACUUGACAUCGUCCCUU
	CCAAUUACGUACUGCGGCUUU	5′P AGCCGCAGUACGUAAUUGGUU
	GCAACAAGUUCACGCAGAAUU	5′P UUCUGCGUGAACUUGUUGCUU
GalNAc4S6ST (Chst15) (NM_173310.3; AB086953.1)	CGAGCAAGAUGAAUAGGAUUU	5′-P AUCCUAUUCAUCUUGCUCGUU
	UCAAAUAAAUCCGCCGAUGUU	5′-P CAUCGGCGGAUUUAUUUGAUU
	AUAAAUUCCUUCCGACUAGUU	5′-P CUAGUCGGAAGGAAUUUAUUU
	GACUAUCUCUACUUUGCAAUU	5′-P UUGCAAAGUAGAGAUAGUCUU

Table – 2

Primer sets for qRT-PCR

Gene	Forward Primer	Reverse Primer
HpRT1 (NM_012583.2)	5'-TGT TTG TGT CAT CAG CGA AAG TG-3'	5'-CTG CTA GTT CTT TAC TGG CCA CAT C-3'
C4ST1 (Chst 11) (NM_001108079.1)	5'-CCA CCG CTT GAA AAG CTA CAT-3'	5'-GGT GTT GTA CTT CTG CGT GAA CTT-3'
C4ST2 (Chst 12) (NM_001037775.1)	5'-CAC TGC CCA CTT CTA TCT GCA TA-3'	5'-ATC GGA AGC CAA CAC GTT CT-3'
GalNAc4S6ST (Chst15) (NM_173310.3; AB086953.1)	5'-TGA GAA GCA AGA AGC TTT GAT GAC-3'	5'-CCG CAG GAT CTT CTG AGT GAT C-3'